# Decomposition of N$_2$O over Ni$_x$Co$_{3-x}$O$_4$ Catalyst

Olga Muccioli[a,*], Eugenio Meloni[a], Marco Martino[a], Simona Renda[a], Pluton Pallumbi[b], Federico Brandani[b], Vincenzo Palma[a].

[a]University of Salerno, Department of Industrial Engineering, Via Giovanni Paolo II 132, 84084 Fisciano (SA), Italy.
[b]Campus Innovation Paris, Air Liquide, Chem de la Porte des Loges 1, 78350, Les Loges en Josas, France.
 omuccioli@unisa.it

Nitrous oxide (N$_2$O) was recognized as a strong greenhouse gas that can be reduced by applying post-treatment technologies. N$_2$O catalytic decomposition is considered the most attractive method for N$_2$O abatement due to its easy operation and high efficiency. Among several catalysts, the cobalt-based mixed oxides have been identified as the most performing for this reaction. In this work a Ni$_x$Co$_{3-x}$O$_4$ catalyst was prepared, characterized by means of nitrogen physisorption, X-ray diffraction (XRD), scanning electron microscopy (SEM), and X-ray fluorescence spectroscopy (XRF), and tested in the N$_2$O decomposition reaction in presence of two different reactant mixtures, by using N$_2$O and O$_2$ with two different vol% as reactants, in order to evaluate the effect of the latter on the catalytic behavior.  The results demonstrated that the concentrations of N$_2$O and O$_2$ in the gaseous stream strongly influenced the activity of the catalyst, indeed, by halving the O$_2$ concentration, the N$_2$O conversion increases from 54 % to 79 %. The Ni$_x$Co$_{3-x}$O$_4$ sample resulted a promising catalyst for N$_2$O decomposition reaction of gaseous stream containing up to 5 vol% of N$_2$O, also in presence of O$_2$.

## 1. Introduction

In recent years, growing attention has been paid toward environmental issues, including greenhouse gas (GHG) emissions. The main GHGs induced by human activities are CO$_2$, CH$_4$ and N$_2$O. In particular, the latter persists for a very long time in the atmosphere, up to 120 years, and its greenhouse effect is 2.5 and 310 times larger than that of CH$_4$ and CO$_2$, respectively (Miao et al., 2021). Moreover, it is noteworthy that the concentration of N$_2$O in the earth's atmosphere has registered an increase of more than 10 % compared to pre-industrial levels (Konsolakis et al., 2013). This rising amount of N$_2$O emissions has aroused great global concern, thus, in addition to CO$_2$ control, the N$_2$O abatement is also of great importance for limiting global warming. The main anthropogenic sources of N$_2$O are fertilization, fossil fuel combustion, and several chemical processes, including adipic acid and nitric acid production, in which the exhaust gases plants consist of 20-50 vol% and 0.03-0.35 vol% N$_2$O, respectively (Hu et al., 2021). Among several technologies proposed for the abatement of N$_2$O, such as selective absorption, thermal decomposition, selective catalytic reduction, the catalytic decomposition process is considered the most attractive choice due to its easy operation and high efficiency (Liu et al., 2016). The decomposition of N$_2$O to oxygen and nitrogen (equation 1), is an irreversible exothermic reaction, kinetically hindered by low temperature conditions.

$$2 \text{ N}_2\text{O} \rightarrow 2 \text{ N}_2 + \text{O}_2 \qquad \Delta H_{298k} = -163 \text{ kJ mol}^{-1} \tag{1}$$

N$_2$O is a linear asymmetrical molecule (N-N-O), where the N-N bond order is about 2.7 and that of N-O about 1.6, so the latter is most probable to be broken first. The thermal decomposition requires temperature above 630 °C to obtain measurable conversions, thus the catalyst has an important role in achieving high conversion at lower temperature (Kapteijn et al., 1996).
The reaction mechanism for the N$_2$O decomposition over catalyst could occur through two different reaction routes (Figure 1) that can be summarized in three elementary steps (Yu, 2018), as follows:

$$\text{N}_2\text{O} + ()^* \rightarrow (\text{O})^* + \text{N}_2 \tag{2}$$

$$2(O)^* \leftrightarrow O_2 + 2()^* \text{ (Langmuir – Hinshelwood)} \tag{3}$$

$$N_2O + (O)^* \rightarrow O_2 + N_2 + ()^* \text{ (Eley – Rideal)} \tag{4}$$

In the first stage (2), $N_2O$ molecule absorbs on active vacant site, denoted as $()^*$, that takes away the oxygen atom from the $N_2O$ molecule. The second stage consists in molecular oxygen combination and desorption (3), and it constitutes the rate determinant stage. According to the equation (4), an adsorbed oxygen atom can react with one free $N_2O$ molecule to produce oxygen gas. It must be noted that the latter mechanism can occur on an isolated site, while the previous requires two close active sites to facilitate O-O combination and enhance reaction probability (Lin et al., 2021). Furthermore, considering industrial applications, other reactant gases could be present in the treated stream, such as oxygen. Excess oxygen in the reactant mixture has inhibitory effect on the $N_2O$ decomposition reaction, since the molecular oxygen competes with $N_2O$ to absorb on active sites, making the process even more difficult. It is clear that the composition of the gaseous mixture can strongly influence the reaction rate, thus the catalytic activity.
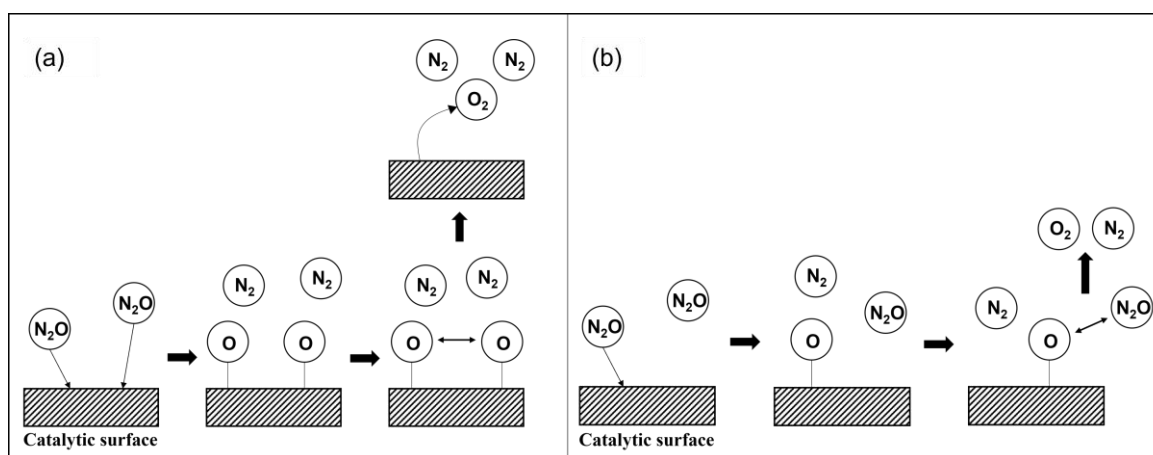


Figure 1: (a) Langmuir-Hinshelwood; (b) Eley-Rideal.

As $N_2O$ catalytic decomposition follows reduction-oxidation mechanism, an effective catalyst consists of at least one metallic ion with variable valences, such as transition metal oxides, supported noble metals, and ion-exchanged zeolites (Li et al., 2016). Among several catalysts active for this reaction, cobalt-based oxides have been especially studied. It is reported that their activity can be enhanced by adding divalent metal into $Co_3O_4$, such as Cu, Mg, Ni or Zn (Abu-Zied et al., 2015), and it has been demonstrated that the introduction of Ni into the structure of $Co_3O_4$ evidently improves the catalytic performance for $N_2O$ decomposition reaction (Yan et al., 2003). Furthermore, mixed valence oxides of transition metals gained wide attention due to the high availability of the elements, low cost, environmental friendliness, ease of preparation and their notable electrochemical activity. Among them, nickel-cobalt combinations exhibit better synergistic effect compared to the corresponding mono-metals (Ashok et al., 2019). In the light of the above considerations, in this work, a nickel-cobalt mixed oxide ($Ni_xCo_{3-x}O_4$) was prepared, characterized, and tested for the $N_2O$ decomposition reaction. In order to evaluate the catalytic performance in severe conditions, the experimental tests were carried out in presence of oxygen. The influence of the reagent mixture composition on the catalytic behavior of the sample was investigated in terms of $N_2O$ conversion by increasing the oxygen concentration from 5 vol% to 10 vol%, keeping unchanged the $O_2/N_2O$ feed ratio. Higher conversions were reached at lower concentrations of $N_2O$ and $O_2$ in the gaseous mixture.

## 2. Experimental

### 2.1 Catalyst preparation

The $Ni_xCo_{3-x}O_4$ oxide was obtained by performing the following procedure. An aqueous solution of $NH_{3,aq}$ (32 vol%) was dropped into a mixed aqueous solution containing known amounts of $(CH_3COO)_2Co \cdot 4H_2O$ and $Ni(NO_3)_2 \cdot 6H_2O$ at room temperature until the pH of the solution reached 9. The resulting precipitate was filtered and washed until neutralizing the filtrate. The obtained samples were dried overnight at 120 °C and calcinated at 600 °C in air for 2 h (10 °C/min heating rate).

## 2.2 Characterization methods

The specific surface areas (SSA) were measured by $N_2$ adsorption at -196 °C, by means of NOVAtouch sorptometer, applying BET method. The same technique was also used for determining the pore volume and pore radius of the sample. The chemical composition of the sample was determined with an X-ray fluorescence spectroscopy (XRF) by means of Thermo-Scientific QUANT'X, based on an energy dispersion analysis. SEM (scanning electron microscopy) observations of the catalytic sample were performed by using Philips Mod.XL30 electron microscope, coupled to an Energy Dispersive X-ray Spectrometer (EDS) Oxford. X-ray diffraction (XRD) patterns were recorded on a Brucker D2 diffractometer, designed according to the Bragg geometry.

## 2.3 Catalytic decomposition of $N_2O$

$N_2O$ decomposition was carried out by means of a properly set up laboratory plant. The experiments were carried out in a tubular fixed-bed reactor located in a furnace for the heating supply. The furnace was provided of three heating sections, each with a dedicated K-type thermocouple and managed by TLK38 controllers, aiming at assuring an optimal thermal profile inside the reactor. The catalyst (1.5 g) was placed in the middle section of the reactor with a powder granulometry of 180-355 μm, previously identified as optimal for limiting the diffusive mass transfer phenomena, so allowing the total exploitation of the catalytic mass (Palma et al., 2016). Two K-type thermocouples in correspondence of the inlet and outlet section of the catalytic bed ensure the monitoring of the temperature. The gaseous stream was fed to the reaction section by means of mass flow controllers (MFCs). The sample was pretreated in situ by heating the system up to 600 °C (10 °C/min heating rate) in Ar flow. The catalytic activity of the sample was investigated under atmospheric pressure in a temperature range of 350-600 °C by employing two different reactant mixtures: 5 vol% $N_2O$, 5 vol% $O_2$ and balanced Ar, 10 vol% $N_2O$, 10 vol% $O_2$ and balanced Ar. The gas hourly space velocity (GHSV), defined in the equation (5), was 15000 $h^{-1}$. The products were analyzed by means of a QGA mass spectrometer (Hiden Analytical, UK), monitoring m/z ratios of 28 ($N_2$), 30 (NO), 32 ($O_2$), 40 (Ar), 44 ($N_2O$), 46 ($NO_2$). The catalytic performance was evaluated in terms of $N_2O$ conversion (6) and selectivity toward $N_2$ (7).

$$GHSV = \frac{Q}{V_{cat}} \tag{5}$$

$$X_{N_2O} = \frac{F_{N_2O,in} - F_{N_2O,out}}{F_{N_2O,in}} \cdot 100\% \tag{6}$$

$$S_{N_2} = \frac{F_{N_2,out}}{F_{N_2,out} + F_{NO_2,out} + F_{NO,out}} \cdot 100\% \tag{7}$$

Herein, Q denotes the total volumetric flow rate and $F_i$ indicates the molar flow rate of the i-species.

## 3. Results and discussion

### 3.1 Catalysts characterization

Characterizations concerning the textural structure and the chemical composition (XRF) of the $Ni_xCo_{3-x}O_4$ sample are briefly listed in Table 1. The catalyst investigated in this study exhibited a SSA value lower than expected. Indeed, it is reported that the surface area of $Co_3O_4$ oxide is about 4 $m^2/g$, and the partial replacement of divalent metals in $M_xCo_{3-x}O_4$ oxide increases the SSA value (Li et al., 2016). Thus, the presence of nickel in the $Co_3O_4$ structure, should have resulted in a wider surface area. On the contrary, the limited surface area and the low porosity obtained in the sample investigated suggest that the preparation procedure led to a peculiar high compact structure.

Table 1: SSA, pore volume, pore radius, Ni/Co ratio (XRF) of $Ni_xCo_{3-x}O_4$ catalyst

| Sample | SSA ($m^2/g$) | Pore volume ($cm^3/g$) | Pore radius (nm) | Ni/Co ratio |
|---|---|---|---|---|
| $Ni_xCo_{3-x}O_4$ | 4 | 0.006 | 1.7 | 0.8 |

The morphology of $Ni_xCo_{3-x}O_4$ displayed in the SEM/EDX images (Figure 2) is characterized by a filamentous structure. Moreover, the EDX elemental mapping clearly illustrates the uniform distribution of Ni, Co and O throughout the sample and confirms the formation of a nickel-cobalt mixed oxide.

The XRD pattern of the catalyst (Figure 3) exhibits diffraction peaks typical of standard cubic $NiCoO_2$ mixed oxide (JCPDS 10-0188) at 37°, 43°, 62°, 74° and 77° 2Θ values. In addition, two peaks indicating a Ni-Co alloy formation are present (Qazi et al., 2021) at 44,6° and 52° 2Θ values.
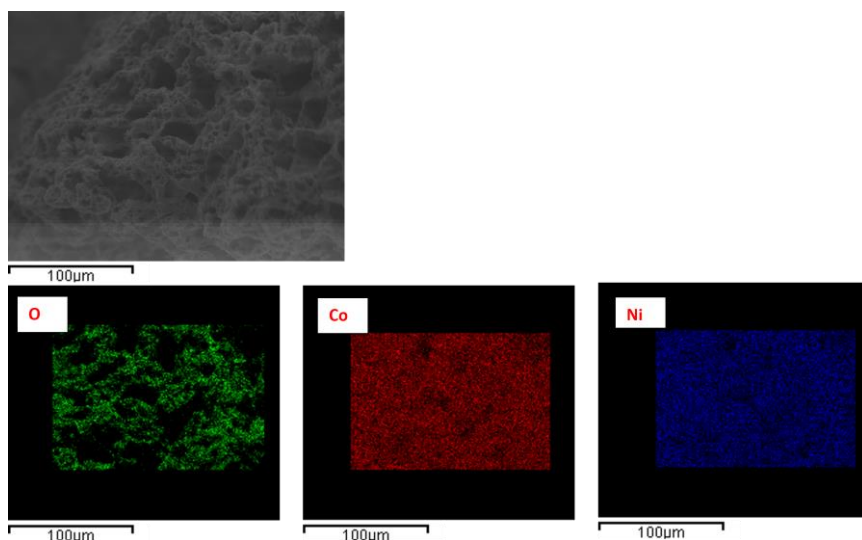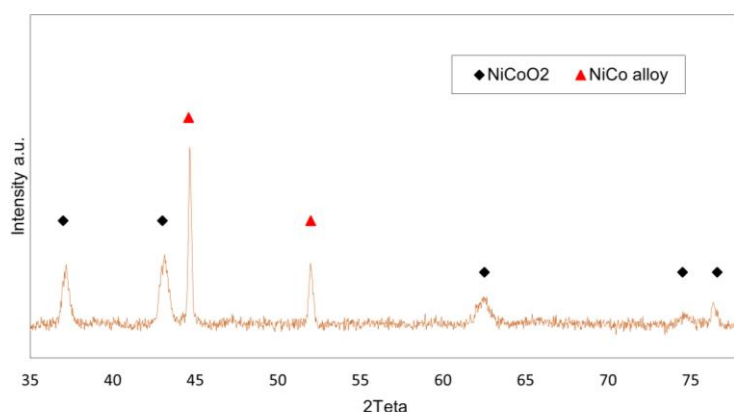


Figure 2: SEM/EDX images of $Ni_xCo_{3-x}O_4$ catalyst



Figure 3: XRD pattern of $Ni_xCo_{3-x}O_4$ catalyst

### 3.2 Catalytic activity of $Ni_xCo_{3-x}O_4$ in $N_2O$ decomposition

The catalytic activity of $Ni_xCo_{3-x}O_4$ in $N_2O$ decomposition in presence of two different feed streams, respectively containing 10 vol% and 5 vol% of $N_2O$, is shown in Figure 4. The total selectivity of the system toward $N_2$ was achieved, confirming that the $N_2O$ was converted without any subproducts, as NO and $NO_2$. The results in terms of $N_2O$ conversion highlights the strong influence of the reactants concentration on the catalytic performance. In the whole temperature range investigated, by halving the $N_2O$ and $O_2$ concentrations from 10 vol% to 5 vol%, keeping unchanged the other operating conditions, higher $N_2O$ conversion values were reached. In particular, the change in $N_2O$ concentration led to a substantial increase in conversion from 54% to 79% at 600°C, at high values of GHSV (15000 $h^{-1}$, similar to the ones of a typical industrial plant). This behavior can be ascribed to the textural properties of the sample combined with the inhibitory effect of the oxygen. It can be expected that increasing concentrations of both $N_2O$ and $O_2$ in gaseous stream limit the reaction mechanism rate over the catalyst surface, where the highly compact structure and low porosity hinder

the interaction of the species with the active sites. As result, the high concentration of the reactants combined with the peculiar textural properties of the catalyst make the $N_2O$ decomposition unfavored.

As explained in section 1, the $N_2O$ decomposition is limited by the first N-O bond cleavage which forms an adsorbed O atom and a gaseous $N_2$, and the second N-O bond cleavage that occurs on the oxygen-occupied site. Site pairs that permit facile adsorbed O atoms migration and combination are required to have high activity. Furthermore, it is reported that to optimize $N_2O$ decomposition rates for applications, the specific reaction routes and site requirements for different catalysts should be considered (Lin et al., 2021). For example, the reaction rate of the catalyst can be enhanced increasing the metal loading to obtain closely spaced site pairs and facilitate O-O combination.

The results obtained from the experimental tests so suggest that the $Ni_xCo_{3-x}O_4$ catalyst could be suitable for the catalytic decomposition of gaseous stream containing up to 5 vol% of $N_2O$, also in presence of $O_2$. Further study may be devoted to the optimization of the operating conditions, in order to increase the catalyst performance in presence of higher concentrations of $N_2O$, typical of tail streams exiting for example from adipic acid production plants (Konsolakis, 2015), as well as to the influence of other typical components of tail gases, such as $H_2O$.
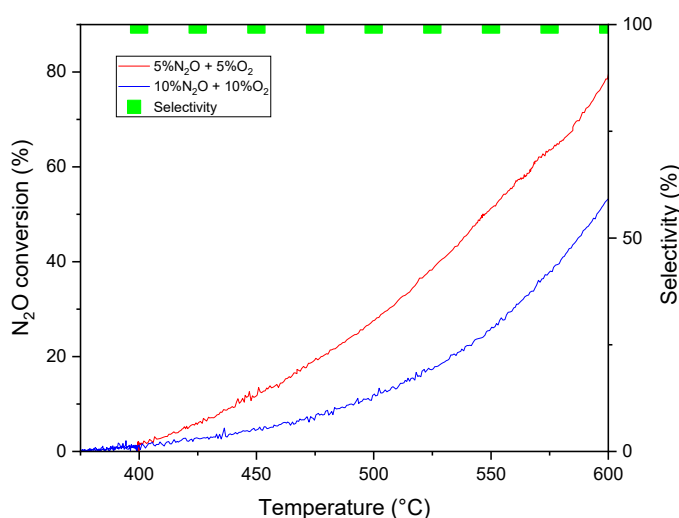


*Figure 4: Activity of $Ni_xCo_{3-x}O_4$ in $N_2O$ decomposition. Operating conditions: GHSV = 15000 $h^{-1}$, 1 atm, feed streams: 10 vol% $N_2O$, 10 vol% $O_2$ and 5 vol% $N_2O$, 5 vol% $O_2$ in Ar.*

## 4. Conclusions

In this work a nickel-cobalt cubic mixed oxide ($Ni_xCo_{3-x}O_4$) was prepared, characterized, and tested for the abatement of $N_2O$. In particular, the performance of the catalyst for the $N_2O$ decomposition reaction was evaluated in presence of oxygen, by varying the $O_2$ percentage from 5 vol% to 10 vol%, keeping unchanged the $O_2/N_2O$ feed ratio and the other operating conditions. The results demonstrated that at lower $O_2$ concentration the $N_2O$ conversion increases from 54 % to 79 %, confirming the inhibitory effect of oxygen. Indeed, as previously explained, since the catalytic cycle is closed by molecular oxygen desorption via Langmuir-Hinshelwood or Eley-Rideal mechanism, the increasing presence of oxygen hinders the adsorption of $N_2O$ on the catalytic surface. Moreover, the textural analysis performed on the catalyst showed that it is characterized by a highly compact structure, thus the low surface area and low porosity limit the availability of the active sites. As result, the high concentration of the reactants combined with the peculiar textural properties of the catalyst make the $N_2O$ decomposition unfavored. Nevertheless, in all the experimental tests and in the whole temperature range investigated (350 – 600 °C), the total selectivity of the system was achieved, without the formation of undesired by-products such as NO or $NO_2$. In conclusion, the results obtained in this work have shown that $Ni_xCo_{3-x}O_4$ cubic mixed oxide allows to successfully treat gaseous stream containing up to 5 vol% $N_2O$, also in presence of oxygen.

**References**

Abu-Zied B.M., Soliman S.A., Abdellah S.E., 2015, Enhanced direct $N_2O$ decomposition over $Cu_xCo_{1-x}Co_2O_4$ (0.0 ≤ x ≤ 1.0) spinel-oxide catalysts, Journal of Industrial and Engineering Chemistry, 21, 814–821.

Ashok A., Kumar A., Ponraj J., Mansour S.A., Tarlochan F., 2019, Highly active and stable bi-functional $NiCoO_2$ catalyst for oxygen reduction and oxygen evolution reactions in alkaline medium, International Journal of Hydrogen Energy, 44, 16603-16614.

Hu X., Wang Y., Wu R., Zhao Y., 2021, N-doped $Co_3O_4$ catalyst with a high efficiency for the catalytic decomposition of $N_2O$, Molecular Catalysis, 509, 111656.

Kapteijn F., Rodriguez-Mirasol J., Moulijn J.A., 1996, Heterogeneous catalytic decomposition of nitrous oxide, Applied Catalysis B: Environmental, 9, 25-64.

Konsolakis M., 2015, Recent Advances on Nitrous Oxide ($N_2O$) Decomposition over Non-Noble-Metal Oxide Catalysts: Catalytic Performance, Mechanistic Considerations, and Surface Chemistry Aspects, ACS Catal., 5, 6397−6421.

Konsolakis M., Aligizou F., Goula G., Yentekakis I.V., 2013, $N_2O$ decomposition over doubly-promoted $Pt(K)/Al_2O_3–(CeO_2–La_2O_3)$ structured catalysts: on the combined effects of promotion and feed composition, Chem. Eng. Journal, 230, 286-295.

Li Z., Cang-cang W., Xiu-feng X., 2016, Catalytic decomposition of N2O over Mg-Co and Mg-Mn-Co composite oxides, Journal of Fuel Chemistry and Technology, 44, 1494-1501.

Lin F., Andana T., Wu Y., Szani J., Wang Y., Gao F., 2021, Catalytic site requirements for $N_2O$ decomposition on Cu-, Co-, and Fe-SSZ-13 zeolites, Journal of Catalysis, 401, 70-80.

Liu Z., He F., Ma L., Peng S., 2016, Recent Advances in Catalytic Decomposition of $N_2O$ on Noble Metal and Metal Oxide Catalysts, Catal. Surv., 20, 121-132.

Miao M., Zhang M., Kong H., Zhou T., Yang X., Yang H., 2021, Progress in Catalytic Decomposition and Removal of $N_2O$ in Fluidized Bed, Energies, 14, 6148.

Palma V., Martino M., Pisano D., Ciambelli P., 2016, Catalytic activities of bimetallic catalysts for low temperature water gas shift reaction, Chemical Engineering Transactions, 52, 481-486.

Qazi U.Y., Javaid R., Zahid M., Tahir N., Afzal A., Lin X., 2021, Bimetallic $NiCo-NiCoO_2$ nano-heterostructures embedded on copper foam as a self-supported bifunctional electrode for water oxidation and hydrogen production in alkaline media, Catalysts, 46, 18936-18948.

Yan L., Ren T., Wang X., Ji D., Suo J., 2003, Catalytic decomposition of $N_2O$ over $M_xCo_{1-x}Co_2O_4$ (M = Ni, Mg) spinel oxides, Applied Catalysis B: Environmental, 45, 85-90.

Yu H., Wang X., 2018, Apparent activation energies and reaction rates of $N_2O$ decomposition via different routes over $Co_3O_4$, Catalysis Communications, 106, 40-43.